HIGH-BRIGHTNESS, FULLY AXISYMMETRIC X-BAND RF GUN †

H. P. Bluem * and A. M. M. Todd
Advanced Energy Systems, P.O. Box 7455, Princeton, New Jersey 08543-7455, U.S.A.

Abstract

Bright, RF photocathode electron guns are the source of choice for most high-performance research accelerator applications. Some of these applications are pushing the performance boundaries of present state-of-the-art guns. A fully axisymmetric X-band radiofrequency electron gun with an upstream power feed has been developed. The present device shows excellent promise in extending the performance of high-brightness sources. Simulations show that it easily breaks the benchmark emittance of one micron for 1 nC of bunch charge when followed by only a short booster accelerator. The pulse length in these simulations is less than 2 ps. While beam testing has not been possible to date, high power RF testing has been performed at a frequency of 11.424 GHz using the Magnicon Facility at the Naval Research Laboratory (NRL). The successful testing proved out the basic design features of the gun with the achievement of a peak cathode accelerating field of 240 MV/m. The simulated electron beam performance details are presented along with the overall design of the gun and the results of the high power RF testing. The same geometry would also lend itself to commercial applications with thermionic cathodes.

INTRODUCTION

Advanced accelerator applications require extremely bright electron bunches that have proved to be a challenge to deliver using extant RF gun designs. An example of this is the LCLS normalized transverse rms emittance specification of less than 1 mm-mrad with 1 nC electron bunches in S-band [1].

The difficulty is partly due to two undesirable features, namely, non-axial-symmetry of the geometry and fields and non-optimal placement of the emittance compensating solenoid [2]. We determined to take the next step in emittance reduction by going to a completely symmetric design that eliminates radial penetrations and thereby also allows optimum placement of the emittance compensation solenoid. Simultaneously, we recognized that X-band could become an emerging market for high-brightness electron guns and decided to design the gun at 11.424 GHz [3].

The input of high RF power is one of the more difficult tasks in accelerator design. At high input RF power, there should be little heat transfer into the cavity and the beam tube, the coupling structure should match the external quality factor and the resultant electric fields should not perturb the electron beam and induce emittance growth. The last requirement is generally satisfied by using two opposed input couplers in the beam tube or an axial input coupler, where the beam tube is an intrinsic part of the coaxial transmission line [4]. In an RF photocathode gun, the annular gap between the cathode and the gun cavity can be used for coaxial RF power input. This has the advantage that the RF field remains axially symmetric and no additional input couplers are needed on the output beam tube. The axial symmetry eliminates transverse kicks to the beam in the vicinity of the couplers that can lead to transverse emittance growth.

DESIGN

Figure 1 shows a schematic cross-sectional view of the normal conducting X–band RF gun with a frequency of 11.424 GHz. This gun has been designed specifically for low emittance at high bunch charge [5]. The cavity has two cells which can be tuned independently.

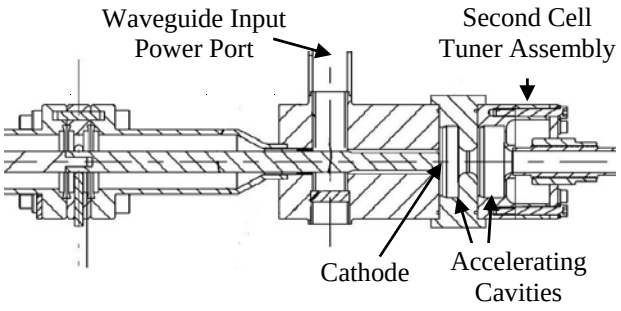

Figure 1: Cross-sectional view of the two cell X-band gun assembly.

All radial structures such as coupling slots, tuning slugs, laser ports, pickup ports, and so on have been eliminated. The cells themselves are of the standard pill-box type. The input power is fed from a rectangular waveguide through a waveguide-to-coaxial adapter. The RF power then travels down the coaxial line and into the cathode cell of the gun. The photocathode is separated by a vacuum gap from the cavity and its surface is in front of the back wall of the first cell. The cathode itself is contained on the tip of the coaxial line center conductor. In the present case, the center conductor is solid copper, however, other photocathode materials or a thermionic emitter could be placed at the tip as alternate cathodes. The center conductor is fixed on the other end to a micrometer. This allows the center conductor, which can be moved ~ 30 microns in the axial direction, to be used for tuning the first cathode cell. For non-metallic cathodes, the center conductor can be fully withdrawn for cathode deposition and processing.

† This work was supported by the US Department of Energy under SBIR grant DE-FG02-01ER83135 and by Advanced Energy Systems.

hans_bluem@mail.aesys.net

A second cell is included in the present design. As usual, the power coupling between cells is through the on-axis iris opening. The second cell also incorporates an axisymmetric tuning mechanism that uniformly pushes and pulls on the end wall of this cell.

The input power coupling mechanism is by nature well suited for strong coupling and has been considered for superconducting guns [6] and high-average-current normal conducting guns [7]. The RF power flows from a rectangular wave guide into a coaxial line which consists of the cathode stalk and the surrounding part of the cavity. The input waveguide can be terminated with a sliding short. This allows the matching of the external quality factor to the required beam power over a certain range. With no external transverse impediments, the bore of the emittance compensation solenoid can be minimized and near optimally located with respect to the gun and cathode, thereby minimizing the delivered transverse emittance [2].

In the case of the present prototype gun, since it is a low-duty-factor X-band design, the coupling had to be limited. One way to achieve this is by setting up the design such that the coaxial line supports a standing wave. To further reduce the coupling, a step was incorporated in the center conductor at the interface between the rectangular waveguide and the coaxial portion. Additionally, the coupling can be controlled through the diameter of the center conductor, allowing for easy post fabrication coupling modification through replacement of the center conductor.

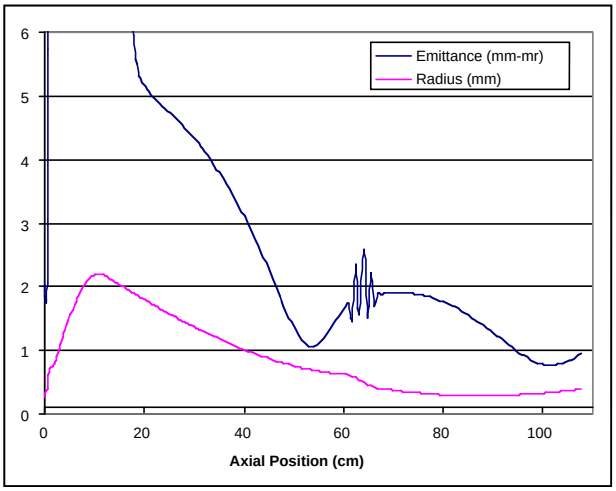

Figure 2: PARMELA beam dynamics calculation for a 1½-cell gun and 4-cell booster to deliver emittance compensation for a 1 nC bunch.

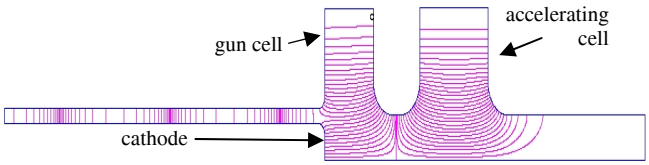

Figure 3: SUPERFISH cavity and coupler fields.

Some results of the numerical simulations of this gun are given in Figures 2, 3 and Table 1. It can be seen that for high bunch charge and short pulse length, a very low emittance is obtained.

Table 1: Analytic results.

Parameter	Low Charge	High Charge (with short booster accelerator)	Units
Charge	0.10	1.0	nC
Beam Radius	0.28	0.34	mm rms
ε_{xn}	0.165	0.764	mm-mrad
Bunch Length	1.0	1.9	ps rms
Energy Spread	1.3	1.5	%
Energy	3.3	8.7	MeV

The SUPERFISH [8] and 3D MAGIC [9] calculations for this concept show that the coaxial portion has standing waves and is part of the resonant circuit. The input coupling occurs at the waveguide-to-coax transition. The axial and radial fields are shown in Figures 4 and 5 repectively.

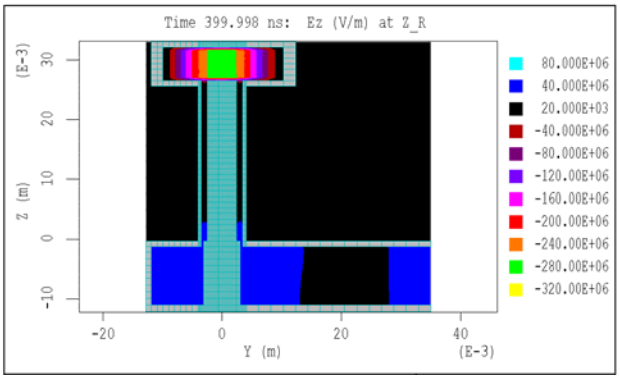

Figure 4: MAGIC calculation of the axial electric fields.

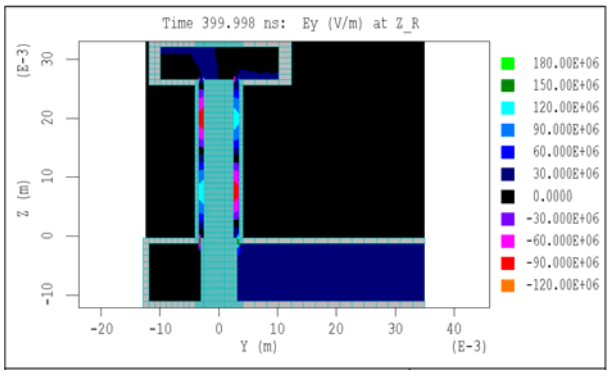

Figure 5: MAGIC calculation of the radial electric fields.

In Figure 6, we show an exploded view of the low power (cold) model of this gun which was used to finalize the gun design and fabrication details. The red pen at the top center of the figure provides an indication of the scale. The two rings below the pen are the accelerating cavities, and the object to the right of the cavities is the end-cell tuning mechanism. The waveguide input arm can be seen to the immediate left of the pen with a sliding short for low-power model testing located opposite the input waveguide on the lower side of the cold model. The center conductor of the coaxial feed can be seen at the lower left. Figure 7 shows the model assembled with key elements called out.

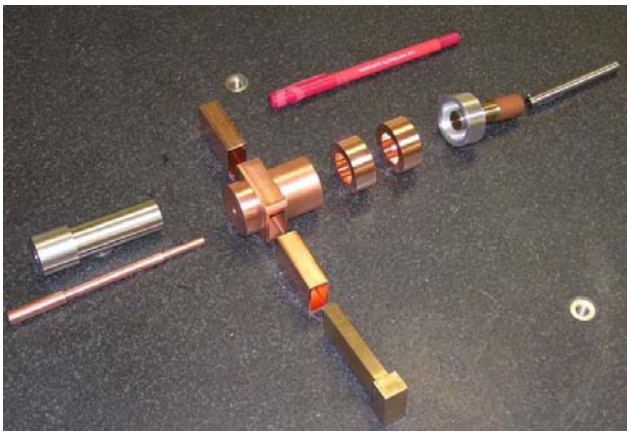

Figure 6: Exploded view of the low power model of the X-band normal conducting gun with a red pen for scale.

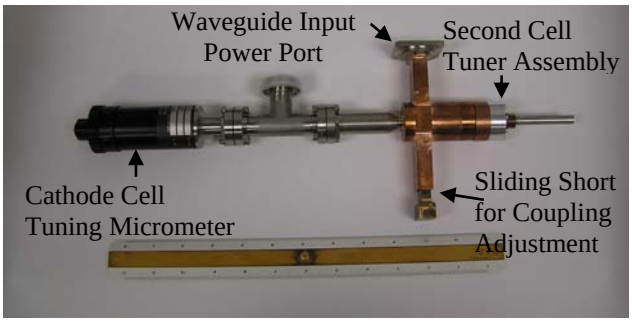

Figure 7: Assembled low power gun model.

This 1½-cell axisymmetric gun is the next step in our development of higher performance injectors with reduced emittance. This is accomplished by eliminating any contributions to emittance growth from non-axisymmetric modes. These modes occur due to coupling slots cut into the accelerating cells and because of slug tuners and sample probes being placed at the outer radius of the accelerating cells. In addition, our design allows optimal placement of the emittance compensation solenoid over a short BNL/SLAC/UCLA-style gun [10]. We achieve this goal by complete preservation of axial symmetry and the elimination of any radial protrusions on the gun body. The microwave feed is brought in through a waveguide-to-coaxial transition and is delivered to the accelerating cells through a coaxial line at the rear of the gun. Axisymmetric tuning mechanisms are designed into the structure for both accelerating cells.

The present design is in X-band at 11.4 GHz, but the overall concept can be scaled to any frequency. Beam dynamics analyses of the gun using PARMELA [11] have shown excellent performance characteristics over a range of bunch charge. The calculations have demonstrated a pronounced advantage (~20%) in being able to place the emittance compensation solenoid over the accelerating structure.

The present design is not intended to operate at CW or very high-duty-factor. Rather it is intended for very high-performance, high-peak-current, low-duty-factor applications such as the LCLS and Compton backscatter sources. Like FZ Rossendorf [6], we are also now considering such coaxial coupling for a high-current L-band superconducting RF gun [12].

TESTING

Low power testing was first performed on the cold model described above. Based on the results of the cold model, the final hot model was fabricated and testing took place at the Magnicon Facility located at the NRL.

Cold Model

The cold model was fabricated from copper and was mostly brazed together so that it could also be used for testing fabrication methods. The assembled cold model is seen in Figure 7.

The photograph shows the linear actuator that controls the center conductor on the left side of the assembly. The second cell tuning mechanism is the aluminum cap seen on the right side of the assembly. The waveguide input flange is seen above the left hand side of the copper body. On the lower side is an adjustable short that is used to adjust the input coupling into the accelerating structure. On the hot model the waveguide short position is fixed. Using this cold model, measurements were made of the cell 1 frequency, cell 2 frequency, coupling into cell 1, and tuning mechanisms for cells 1 and 2. These measurements were compared to calculations made using SUPERFISH and are presented in Table 2.

Table 2: Cold test results compared to calculations.

	measured	**calculated**	
cell 1 frequency	11.390	11.385	GHz
cell 1 tuning	4	6	MHz/mil
cell 2 frequency	11.234	11.193	GHz
cell 2 tuning	6	5.5	MHz/mil

The measured numbers agree quite well with the calculations. The largest discrepancy was in the cell 1 tuning, which was determined to be due to differences in the corner radius at the outer edge of the inner conductor. A larger corner radius on the end of the center conductor results in a decreased tuning rate. These tuning rates are sensitive enough to make up for relatively large final assembly frequency errors while still allowing sufficiently fine tuning.

Hot Model

The prototype X-band gun, whose RF surfaces were electropolished, is shown in Figure 8. Due to time and program constraints, a set up for electron beam testing could not be accomplished. Thus, the hot model testing was confined to high power RF testing.

Tuning of the hot model proceeded smoothly, and post-braze fine-tuning was readily accomplished using the built-in mechanisms. The only issue that arose was the input coupling, whose final value was close to 0.5 due to the measured Q being lower than predicted.

Although the design flexibility of the gun afforded the potential to install a modified center conductor to provide for increased input coupling, programmatic timing

considerations did not permit this. When final tuning was completed, the gun assembly was baked and transported to the test facility.

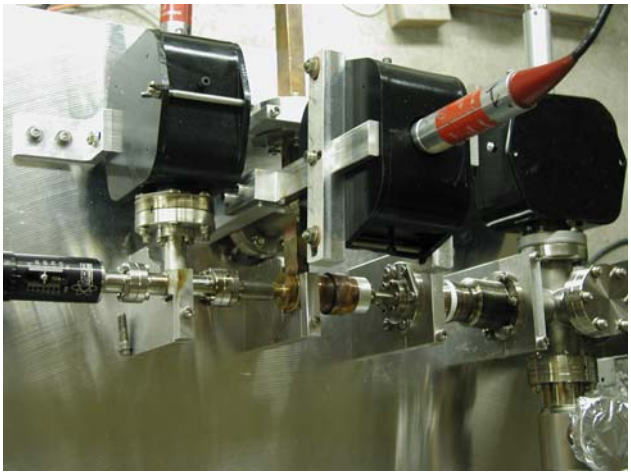

Figure 8: Prototype X-band gun.

Due to the lower coupling obtained in practice, high power tests were performed with the second cell detuned in order to provide a better input match. This also delivered more power to the cathode cell.

Figure 9 contains a series of oscilloscope plots showing the modulator pulse, the forward power in both arms of the magnicon output, and the reflected signal from the gun. Tests showed that the matched arm of the magnicon was not affected by the gun mismatch.

Testing started with a relatively long magnicon pulse, shown in Figure 9a, but this limited the repetition rate to one to two pulses per second due to system considerations. Under these conditions, conditioning proved to be too time consuming. Shortening of the magnicon modulator pulse, shown in Figure 9b, did not substantially affect the RF pulse but allowed the repetition rate to be increased up to six pulses per second. Figure 9c shows an example of a breakdown event.

The conditioning history of the gun is presented in Figure 10. Conditioning proceeded quite rapidly to above 200 MV/m. Consistent operation was achieved at 240 MV/m, and the maximum gradient reached was 255 MV/m. Conditioning was terminated early on the third day.

After conditioning, the center conductor of the coaxial input coupler was removed from the system for inspection. Evidence of breakdown was clearly evident as anticipated. The interior of the gun itself could not be inspected due to the small tubes, but it is expected that virtually all of the breakdown occurred in the coaxial feed section. Photos of the inner conductor of the coaxial feed are shown in Figure 11.

It is evident from this figure that the breakdown was not azimuthally symmetric indicating that the center conductor was not exactly centered. There are three regions of breakdown. The region of breakdown seen in the center of both photographs occurs at the step in the rod that was placed at the interface between the

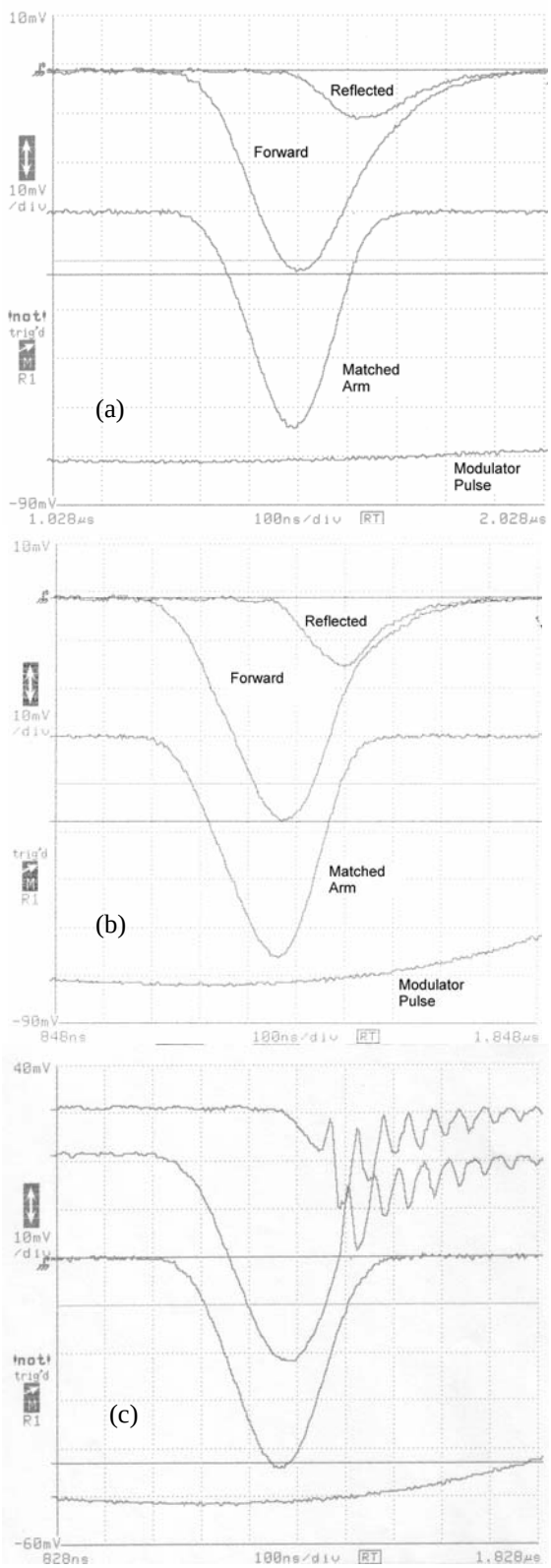

Figure 9: Forward and reverse power in the gun arm and forward power in the orthogonal arm of magnicon for a) a long modulator pulse, b) a short modulator pulse, and c) showing a breakdown event. Note in c) that the matched, orthogonal magnicon arm is not affected by the breakdown in the gun.

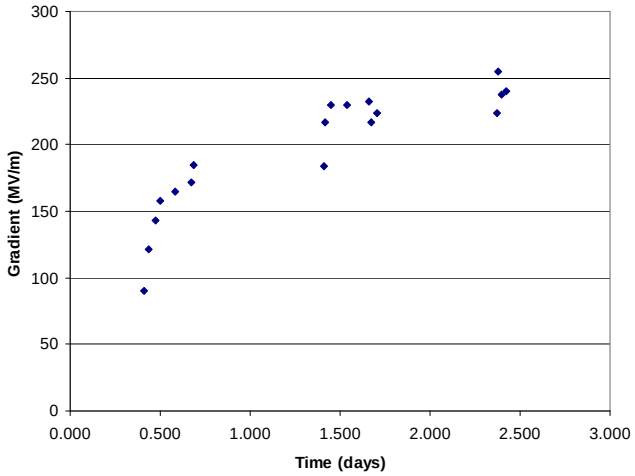

Figure 10: Conditioning history of the gun showing the calculated gradient as a function of time.

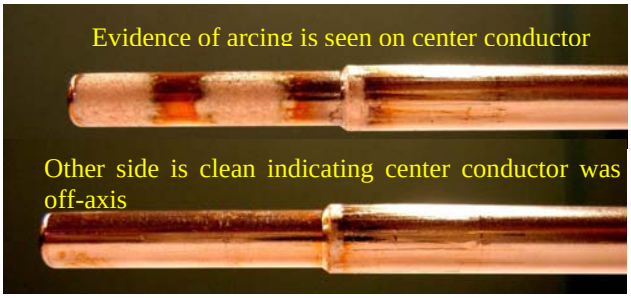

Figure 11: Center conductor photos after conditioning.

waveguide and the coaxial line. This breakdown occurred over the full 360 degrees around the conductor, but was concentrated to one side due to the probable misalignment. The step was placed in the line to reduce the coupling but actually proved unnecessary, since the final input coupling was too low. It is easily removed in future designs which will benefit from the increased coupling. A slight overcoupling is actually preferred in pi-mode RF guns to improved the fill time and to reduce the fill transients that overcoupling generates.

The other two regions of breakdown are only evident in the upper photo of Figure 11. The other side of the center conductor shown in the lower photo is still clean, which is a clear indication a misaligned center conductor. The two breakdown regions correspond to the peaks of the standing wave pattern in the coaxial section. The standing wave minimums do not show any evidence of breakdown. Future work should include simulations of the effect of center conductor misalignment. For a standing-wave design of this type, an optimization study to reduce the field levels in the coaxial region so as to minimize the breakdown effects of any misalignment, would also be useful. High coupling factor designs that can utilize a traveling wave in the coaxial portion should not suffer from breakdown in this region.

A very important positive indication is the lack of breakdown evidence at the tip of the center conductor, the edges of which can be seen in Figure 11. The radius on the corner still appeared clean as did the face of the center conductor end, which is the cathode surface. The lack of breakdown in this area is a positive indication that the overall concept is capable of higher gradients than achieved during this testing.

CONCLUSIONS

In an RF gun with a vacuum gap that separates the cathode from the surrounding cavity, the gap can be used for coaxial input of RF power with many significant advantages. The patented gun design (US Patent No. 7,116,064) incorporates full axial symmetry in order to eliminate any emittance growth from higher order multipole RF fields and to allow optimal placement of the emittance compensation solenoid. The rear input coupling feed also allows isolation of the cathode from the main gun body eliminating RF power leakage into the coaxial coupling line and opens up the downstream area to diagnostics, magnetics and laser ports. The fabricated gun contains 1.6 cells, utilizes coaxial coupling from the upstream end of the unit and allows for axisymmetric tuning of both the cathode cell and the second accelerating cell. Although the present design is at 11.424 GHz, the basic design features are scalable to any frequency and differing cathode concepts. The features of the gun have been proven to operate at high gradient.

ACKNOWLEDGEMENTS

The authors would like to thank Steve Gold and coworkers at the NRL Magnicon Facility for their help and flexibility during the high power testing. This X-band gun concept is protected by US Patent No. 7,116,064.

REFERENCES

[1] R. Akre et al., "Commissioning the Linac Coherent Light Source Injector," PRST-AB 11, 030703 (2008).
[2] B. E. Carlsten, "Photoelectric Injector Design Code," *Proc. PAC 1989 Chicago, Il, USA*, IEEE89CH2669-0 (1989) 313.
[3] e.g. See X-band application papers in these Proceedings.
[4] K. Abrahamyan et al., Nucl. Instr. and Meth. **A528** (2004) 360.
[5] H. P. Bluem et al., "Electron Injectors for Next Generation X-Ray Sources," *Proc. SPIE*, **5534** (2004) 132.
[6] D. Janssen, V. Volkov, H.P. Bluem, and A.M.M. Todd, "Axial RF Power Input into Photocathode Electron Guns," *Proc. PAC 2005 Knoxville, TN, USA*, ISBN 0-7803-8860-7 (2005) 743.
[7] R.A. Rimmer, "A High-Gradient CW RF Photo-Cathode Electron Gun for High Current Injectors," *Proc. PAC 2005 Knoxville, TN, USA*, ISBN 0-7803-8860-7 (2005) 3049.
[8] http://laacg1.lanl.gov/laacg/services/download_sf.phtml
[9] http://www.mrcwdc.com/magic/index.html
[10] X. J. Wang et al., *Proceedings of the 1998 LINAC Conference*, ANL-98/28 (1998) 866.
[11] http://laacg1.lanl.gov/laacg/services/parmela.htm
[12] A.M.M. Todd, "State-of-the-Art Electron Guns and Injector Designs for Energy Recovery Linacs (ERL)," *Nucl. Instr. & Meth A* **557** (2006) 36.